Journal of Theoretical and Applied Information Technology
15st July 2026. Vol.104. No.13
© Little Lion Scientific
ISSN: 1992-8645 www.jatit.org E-ISSN: 1817-3195

POLYCYSTIC OVARIAN SYNDROME PREDICTION USING AN EFFICIENT NEURAL NETWORK-BASED LEARNING MODEL

[1]B. BAZEER AHAMED, [2]KALAICHELVI NALLUSAMY, [3]NANDHAGOPAL SUBRAMANI, [4]V. JEMMY JOYCE, [5]J. ALFRED DANIEL, [6]K. ARUNKUMAR, [7]P. SHERUBHA

[1]University of Technology and Applied Sciences, College of Computing and Information Sciences Al Musannah, Sultanate of Oman.
[2]Assistant Professor, Department of Information Technology, Sri Sivasubramaniya Nadar College of Engineering, Kalavakkam, Chennai, India.
[3]Assistant Professor, Department of Computer Science and Engineering (Artificial Intelligence and Machine Learning), K P R Institute of Engineering and Technology, Coimbatore.
[4]Assistant Professor, Mathematics, Karunya Institute of Technology and sciences, Coimbatore, India.
[5]Department of Computer Science & Engineering, Karpagam Academy of Higher Education, Coimbatore, India.
[5]Centre for Immersive Reality and Gaming, Karpagam Academy of Higher Education, Coimbatore, India.
[6]Associate Professor, Department of Computer Science Engineering, RVS Technical Campus-Coimbatore.
[7]Associate Professor, Master of Computer Applications, Karpagam College of Engineering, Coimbatore.
Mail id: [1]ahmedbazeer40@gmail.com, [2]kalaichelvin@ssn.edu.in, [3]nan.ecs1@gmail.com , [4]jemmy@karunya.edu, [5]85.alfred@gmail.com, [6]arun1148@gmail.com, [7]sherubha0106@gmail.com

ABSTRACT

Polycystic ovarian syndrome (PCOS) is a hormonal disorder diagnosed during a woman's reproductive years. Several techniques exist to detect PCOS, but few methods address the combination of mental health issues with PCOS. This proposed system features an automated early detection model that assesses the likelihood of both PCOS and mental health problems accurately. Many individuals respond in natural language during real-life applications to share their health status in response to clinician inquiries. The underlying linguistic structure, which links symptomatic manifestations to the diagnostic process of Polycystic Ovary Syndrome, is exploited through a learning-based modelling paradigm. This approach is called Bounding-box based Convolutional Neural Networks (BB-CNN). The model effectively learns and extracts the most influential features to improve prediction accuracy. The proposed BB-CNN achieves 97.34% accuracy and 96.01% precision, recall, and F-measure. Various statistical measures are evaluated and compared with other methods.

Keywords- *PCOS, Hormonal Disorder, Deep Learning, Convolutional Neural Networks, Bounding Box, Statistical Measures*

1. INTRODUCTION

A hormonal disorder primarily identified in adolescent females and in the generative stage of women is referred to as polycystic ovarian syndrome (PCOS). This is a general and prevalent illness that has various phenotypes that have various presentations [1]. Various existing approach discovered PCOS primarily. PCOS affects around 6-26% of women, according to the WHO. The failure of ovulation and infertility are included with difficulties of mental health. There are various impacts created by the PCOS that range from acne to obesity, creating improper menstruation and infertility that leads to the difference in life's quality [3]. Using the Rotterdam Consensus, the detection of PCOS can be done, and the people who have PCOS must face at least these two circumstances that are mentioned based on the study. They are (i) Ovulation absence, (ii) indication of hyperandrogenism, and (iii) Ovaries gets infected due to polycystic. There are various impacts created by PCOS like obesity, amenorrhea, metabolic impairment, cardiovascular disorders, and type 2 diabetics. The pervasiveness of PCOS can be evaluated between 6 to 26 % that are depicted based on WHO [4]. The PCOS pervasiveness in India ranges from 9.13 to 36% (8). PCOS is considered the major reason for emotional issues and infertility. Around one-third of women have fertility problems due to PCOS. More worries and depression are faced by the women who are having PCOS than the women who do not have

PCOS. The proportion of anxiety and depression in women who are having PCOS is 11-25% and 28-39% accordingly [5]. PCOS has considerable impacts on both emotional and physical health that affect the quality of life based on international studies [6]. Clinical symptoms and irregular ovarian morphology are needed to categorize PCOS conditions. The conditions are fertility related issues, oligo-amenorrhea, obesity, anovulation, unwanted uterine bleeding, and hirsutism [7]. Researchers stated that infertility, disturbances in menstruation, and hyperandrogenism are the results of multi-factorial endocrine disorder. The guideline cause of PCOS needs to be solved due to the multi-factorial complications in spite of improved diagnostic advancements and improved infrastructures. Hyperandrogenism, oligo-amenorrhea, and polycystic ovaries are the characteristics of PCOS. First, the cause of these measures needs to be discussed [8]. Jones et al. [9] state that hyperandrogenism is caused because of adrenal increases or production of ovarian androgen. Likewise, due to the menstrual time period being more than 35 days (>35 days), oligo-amenorrhea is caused. Because of the absence of menstrual bleeding for more than three months (> 90 days), amenorrhea is caused. Pelvic sonography is the most useful diagnostic process, which is a defensive, safer and quick diagnostic approach to visualize the ovarian.

Legro et al. [10] states that women's health conditions are very important, and the execution of different effective techniques needs to be reinforced for the health system based on the recommendations mentioned by the WHO that benefits each individual. It is not aware of how the health systems need to be handled and structured prominently to provide a correct answer to the particular needs of the women and adults to those who are more endangered and poorest between them [9]. Henceforth, the consideration can be modelled to give a good call for the analysis of PCOS that are monitoring the conditions of women's health and needs to be addressed the difficulties systematically that are found between women and adults in protecting the health conditions that are stated. This system is related to the essential actions which are needed to improve the conditions of women's health that improve the women's health conditions [10]. The women's health condition is very important to each woman, their family, and society. Then, these conditions of women's health move to the country's next level. The detection of PCOS can be done with the help of biochemical examinations like examinations of the hormone and blood tests, but it is a costly examination [11] – [12]. The detection of PCOS is done by an ultrasound scan which is shown by the latest research. Here the doctor calculates the follicles numbers in the ovaries and their size. PCOS can be predicted using clinical factors like length of menstrual cycle and BMI. Moreover, this evolves clinical acumen and distinction of a clinician; also an invasion of women's privacy, and this is not an automated process, and women's mental health is not observed [13] – [15]. Different techniques are suggested to identify PCOS in the literature. These are widely classified into two sections.

a. With the help of different statistical tools like χ two and Fisher's exact test, the relationship between PCOS and mental health is examined related to studies. Moreover, there is no consideration about PCOS diagnosis and the relevant accuracies.
b. The researchers intended to detect PCOS with the help of image processing approaches and deep learning algorithms. But the emotional health and psychological health are not observed.

The present study helps to include both psychological and clinical factors to overcome the mentioned demerits of the previous system in detecting and diagnosing the possibility to have PCOS and related emotional health problems. Conventional machine learning algorithms are not used to model the system beneath observation since the relevant psychological and clinical data to PCOS can be differed from one woman to another and evolve intrinsic unreliability, ambiguity, and imprecision. Rather than the conventional algorithms like K-Nearest Neighbours (K-NN), D-tree and SVM, the fuzzy algorithms like fuzzy approach for the preference order with the help of similarity to the absolute results and fuzzy AHP are used to determine the efficiency and robustness.

2. RELATED WORKS

Sarfraz et al. [16] conducted an exhaustive and systematic survey that indicates that PCOS is interlinked with psychological problems or emotional health problems like depression, worries, dissatisfaction about the body, and eating disorders which lowers the qualities of life. The author did not mention the implicit relationship between mental health and PCOS in the research. The author proposed the efficient treatment of PCOS strongly can able to stabilize the problems of mental health.

A systematic review about physical exercise and mental health with PCOS was conducted [17] and stated that the introduction of physical exercise was able to enhance the qualities of life and women's psychological health. The association linking PCOS with mental health outcomes is established and found endangers and predictors to predict the reasons for the depression in women along with PCOS. The author implemented a study that included women who had PCOS total of 60 in numbers were taken. Those details were provided to the PRIME-MD PHQ, the BDI, and the BAI for the identification of mental health problems. The data were examined to determine the categorical data were statistically assessed. The test shows that 40% of women (24 out of 60) endure depression, and 16.6% of women endure mood disorders and provide about 56.6% of PCOS women have mental health problems.

A systematic review was conducted by Sharif et al. [18] related to geographical ethnicity and location. The pervasiveness of PCOS was found among 6 to 9% in the study over the United Kingdom, United States, Asia, Greece, Australia, Spain, and Mexico related to diagnostic criteria of the National Institutes of Health (NIH). This research proposed that no influence of racial or no influence of ethnicity is there over the pervasiveness of PCOS. Smooth et al. [19] executed the pervasiveness of PCOS in grown women. Begg's tests were utilized for checking the bias in publication, and 12 published articles were taken in the author's meta-analysis. The PCOS in the population of adults was around 11.04% depending on Rotterdam basis, 3.39% depends on NIH basis, and 8.03% depends on an excess of androgen. The society of PCOS was proved with the help of 477 participants and the software of STATA. The relationship between PCOS and emotional health is examined the lack of exercise, what motivates women, and who helps them stay active who have or do not have PCOS in the research of Uyar et al. [20]. The author concluded that women who have PCOS needs more support when compared with women who are not having PCOS using a statistics calculation and the local database. Likewise, ADHD and ASD investigated by Vierira et al. [21] and these are proved that the prevalence of ADHD and ASD is greater in PCOS mothers having children. The association of PCOS along with psychiatric morbidity is investigated by Welt et al. [22] in the same development, and these affect the quality of life. The author can associate PCOS along with psychiatric morbidity using binary logistic regression.

The detection of PCOS is examined by some studies with the help of computational and machine learning algorithms. The phenotypes of PCOS are compared by Yanez et al. [23] in the latest development having a view of the metabolic profiles in the hormone, clinical and the varied answers to clomiphene. The author achieved individuals afflicted with advanced-stage PCOS (phenotype A classification) exhibit an elevated susceptibility to metabolic dysregulation and cardiovascular pathologies than others using descriptive statistics. Then the phenotype division can able to help the patients with the accurate diagnosis is concluded. Zandi et al. [24] conducted the latest calculation study states that earlier PCOS detection and prediction model was suggested. This model achieved 89.02% accuracy in a random forest classifier. The author took the 541 women, each described by 23 characteristics covering clinical and metabolic measures. Likewise, Yildiz et al. [25] investigated that 119 women with 18 features were considered with clinical variables to determine PCOS and achieved 97.65% accuracy with the help of the Naïve Bayes classifier. A study is done with 84 women with 13 features were considered to identify PCOS and achieved the 94% of accuracy with the help of artificial neural networks. The author conducted a study that states the imagining parameters like follicles with clinical and biochemical variables like BMI and hormonal levels to detect the PCOS and achieved the accuracy of 95% with the help of a support vector machine (SVM). The author conducted a study that states that fuzzy logic is the most efficient computing method for computing human cognitive abilities. The medical data can be categorized and are described clearly in this proposed system. Furthermore, how fuzzy TOPSIS can be utilized broadly is described for trusted health care development software. None of these researches has studied mental health in the investigation. The data was achieved in all the research through taking the interview with women and from the laboratory. Since the possibility of acquiring PCOS is based on various variables and also like the features of data are undetermined, the fuzzy algorithms are best suited than the crisp algorithms.

3. METHODOLOGY

The foremost objective of this chapter is to design a predictor model for polycystic ovarian syndrome (PCOS) using a learning approach. The benefits of Deep Learning (DL) methods have paved the way for PCOS prediction by learning changes from previous histories. Various existing techniques examine PCOS severity from the laboratory, clinical, and clinical examinations. This work concentrates on presenting an enhanced feature selection for attaining a global solution, thereby improving the reliability and efficiency of the predictor model. The feature selection approach is made with an extensive literature study in designing a predictor model for PCOS medical applications.

3.1. Dataset Description

Here, Ultrasound images are used for analysis. The available online dataset consists of ultrasound images of ovaries prepared with the help of medical experts and Gynaecologists for follicle prediction with soft computing techniques. The images are captured using transvaginal ultrasound transducers operating at 26 Hz. Some images are attained from sources. It includes 80 ultrasound images with 256 * 256 sizes, 30 normal ovaries, 30 PCOS, and 20 IC ovaries.

Table 1: Summary of existing ML approaches for disease diagnosis

Author	Method	Goal	Merits	Demerits
Jones et al., [16]	Least Squares Kernel and N.N.	Use ML techniques for examining Electromyography Patterns	The least Square Kernel gives superior prediction accuracy compared to prior approaches.	Classification remains unsolved.
Legro et al., [10]	Supervised ML and Logistic Regression	To predict risk factors	vulnerable factors interaction	Lesser classification accuracy
Moschos et al., [12]	DT and Markovian models	Analysis of diverse prediction models to elucidate the constraints.	Provides optimal decisions during the decision making	Not appropriate for a multi-valued class.
Peng et al., [13]	N.N.s	Prediction	Accountable for prediction	Accuracy has to be enhanced.
Perry et al., [14]	Integration of Cuckoo Search and Adaboost	Prediction with ensemble model	Provides higher prediction accuracy compared with prior approaches.	Very low sensitivity.
Sharif et al., [18]	Adaboost Classifier	Fibromyalgia and psychopathological feature classification	Diminishes pointless tests to save time and cost.	Lesser prediction accuracy.

3.2. Pre-Processing

PCA helps you see multivariate data in 2D/3D, making it easier to find trends, big changes, groupings, and weird points. This summary can show connections between data points AND between the factors you're measuring. Take into consideration the image dataset denoted as 'X', wherein 'm' rows correspond to the dataset comprises variables, with 'n' columns corresponding to distinct individual land cover observations, The resultant matrix, comprising 'm' row vectors each of length 'n', is formulated as Eq. (1):

$$X = \begin{bmatrix} x_{1,1} & x_{1,2} & \dots x_{1,n} \\ x_{2,1} & x_{2,2} & \dots x_{2,n} \\ \vdots & \vdots & \vdots \\ x_{m,1} & x_{m,1} & \dots x_{m,n} \end{bmatrix} = \begin{bmatrix} X_1 \\ X_2 \\ \vdots \\ X_m \end{bmatrix} \qquad (1)$$

ISSN: 1992-8645 www.jatit.org E-ISSN: 1817-3195

As stated in Eq. (2), the pattern requires the matrix X, representing a linear transformation into $Y_{(m,n)}$ using $P_{(m*m)}$ with row variables $p_1, p_2, \ldots, p_m$ and column vectors $x_1, x_2, \ldots, x_n$.

$$Y_{m*n} = P_{m*m}\,X = \begin{bmatrix} p_1.x_1 & p_1.x_2 & \ldots p_1.x_n \\ p_2.x_1 & p_2.x_2 & \ldots p_2.x_n \\ \ldots & \ddots & \ldots \\ p_m.x_1 & p_m.x_2 & p_m.x_n \end{bmatrix} \quad (2)$$

Here, proj(X), the projection transform of original dataset X onto the column vector P is specified here by p_i. 〖 x〗 _j. The directional vectors corresponding to the principal components are represented here by Prows. By anticipating directions with highest assessing variance and leveraging directional insights to delineate novel investigative trajectories, PCA takes into account assesses dataset variance and pursues orthogonalization of feature interdependencies. To do normalization and weighted analysis, the initial step in Principal Component Analysis (PCA) entails centring the dataset by subtracting mean values. Equation (3) expresses it as follows:

$$X_{i,j} = Z_{i,j} - \overline{X}_j \quad (3)$$

The standardized dataset is denoted by $X_{(i,j)}$, the standardised value of variable j for the i-th sample is represented as $Z_{(i,j)}$ and the sample means for variables j are specified by (X_j)̅. All likely off-diagonal elements representing inter-variable covariances and diagonal entries indicating individual variable variances are regarded as all the variables, and the covariance between variables is used to indicate how correlated they are Equation (4) expresses it as follows:

$$C_x = \frac{1}{n-1} XX^T = \frac{1}{n-1} \begin{bmatrix} x_1x_1^T & x_1x_2^T & \ldots x_1x_m^T \\ x_2x_1^T & x_2x_2^T & \ldots x_2x_m^T \\ \vdots & \ddots & \vdots \\ x_mx_1^T & x_mx_1^T & \ldots x_mx_m^T \end{bmatrix} \quad (4)$$

While lesser values indicate the system noise, considerable deviations are typically crucial since they are connected to certain system dynamics. Covariance C_γ of the converted matrix Y_(m*n) must therefore meet a few prerequisites: 1) The diagonal entries are maximized to maximize the signals, and 2) the off-diagonal entries are reduced to lower the covariance among the variables. The transformation matrix P, of dimension m×m, comprising vector elements p_1, p_2,..., p_m satisfies the aforementioned requirements since C_γ is structurally similar to a diagonal matrix, wherein, as seen in Eq. (5):

$$\begin{aligned} C_\gamma = \frac{1}{n-1} YY^T &= \frac{1}{n-1} (PX)(PX)^T \\ &= \frac{1}{n-1} (PX)(P^TX^T) \\ &= \frac{1}{n-1} P(XX^T)P^T \\ &= \frac{1}{n-1} PST^T \end{aligned} \quad (5)$$

In this case, the squared symmetric matrix is diagonalized by (XX^T)^T=XX^T, and the symmetric S_(m*m) is represented as in Eq. (6):

S = E D E^(-T) (6)

In this case, D represents a matrix wherein the diagonal elements correspond to the eigenvalues of S, and E denotes an m×m matrix comprising eigenvectors of S as its column vectors. Eigenvectors in the row matrix are represented by P=E^T. Consequently, the covariance matrix pertaining to γ is presented in Equation (7)

$$C_\gamma = \frac{1}{n-1} PSP^T = \frac{1}{n-1} E^T (EDE^T)E = \frac{1}{n-1} D\,;\text{where } EE^T = I; I \rightarrow m*m \quad (7)$$
Identity matrix

The matrix that shows how variables covary pairwise is rewritten as the matrix product of the eigenvectors and their transposed counterpart multiplied by the sum of Ψ eigenvalues. Each principal component satisfies the following criteria and is regarded as a linear aggregate of the designated x variables, formed via weighted summation, utilising given coefficients. These are: 1) maximising Y variance; 2) certain a linear aggregate of the designated x variables, formed via weighted summation, utilising given coefficients; and 3) the newly derived principal components exhibit zero correlation with those principal components identified in preceding iterations. Assume that the covariance matrix C_gamma possesses eigenvalues lambda_1, ..., lambda_t, arranged in strictly decreasing order: lambda_1 > lambda_2 > ... > lambda_t. Consequently, the proportion of total variance attributable to the i-th principal component is denoted by gamma_i, as given in Equation (8)

$$\frac{\lambda_i}{\lambda_1 + \lambda_1 + \cdots + \lambda_t} \quad (8)$$

To prevent information loss, the proportion of variance accounted for by the k^th principal component ought to be larger or of greater significance, as shown in Eq. (9):

$$\frac{\lambda_1 + \lambda_2 + \cdots + \lambda_k}{\lambda_1 + \lambda_2 + \cdots + \lambda_t} = 1 \quad (9)$$

3.3. Feature Reduction with L1 and L2 Norms

Feature reduction results in jobs requiring less computing time and storage capacity or fewer resources to finish computations. The approach utilises L1 regularisation, commonly referred to as Lasso Regression, alongside L2 regularisation, more commonly known as Ridge Regression. The Ridge Regression methodology integrates a penalisation component within the objective loss function equating to the squared magnitude of the coefficient, in contrast to Lasso Regression, which incorporates a penalty term corresponding to the absolute value of the coefficient's magnitude. Some current methods, such as the graph embedding model uses the L2-norm for measuring distances and suffers from two big drawbacks: they are impractical for cysts and do not offer a larger margin due to a larger class distance, which weakens the tiny class distance. L1 and L2 norms based on discriminant projection thereby improve classification performance. The model maximizes the goal function in an effort to forecast the best projection. Equation (10) expresses it as follows:

$$w_{opt} = \arg\max_{w^T w=1} \frac{\sum_{i,j=1}^{c} B_{ij} \left\| w^T (m_i - m_j) \right\|_2^2}{\sum_{k=1}^{c} \sum_{i,j=1}^{N_k} A_{i,j}^k \left\| w^T (x_i^k - x_j^k) \right\|_2^2} \quad (10)$$

The definitions of B_ij and A_(i,j)^k are as follows: B_ij=exp 〖(-|(|m_i-m_j |)|^2/s)〗 and The element A_(i,j)^k is given by the expression exp(-|(|x_i^k-x_j^k |)|^2/t). Subsequently, m_i and m_j denote the mean vectors of the i-th and j-th classes, respectively, whereas t>0 and s>0 indicate the parameter. The model's robustness is enhanced using L1-norm-based discriminant analysis, which is represented by Eq. (11):

$$w_{opt} = \arg\max_{w^T w=1} \frac{\sum_{i,j=1}^{c} B_{ij} \left| w^T (m_i - m_j) \right|}{\sum_{k=1}^{c} \sum_{i,j=1}^{N_k} A_{i,j}^k \left| w^T (x_i^k - x_j^k) \right)} \quad (11)$$

3.4. L_2 Normalization

In the vast margin of lower-dimensional space, the L2-norm decreases the effects of large-class length and its results while increasing the impact of small-class distance. In general, the L2-norm can significantly shorten the distance between the criteria function's data points. It helps improve the model's predictability. It is theoretically represented as in Eq. (12) and is crucial for classification purposes:

$$w_{opt} = \arg\max_{W} \frac{\sum_{i,j} B_{ij}^p \left| w^T (x_i - x_j) \right|_2}{\sum_{i,j} B_{ij}^p \left| w^T (x_i - x_j) \right|_2} \quad (12)$$

The element A_(i,j)^k is given by the expression exp(- |(|x_i^k-x_j^k |)|^2/t). Subsequently, m_i and m_j denote the mean vectors of the i-th and j-th classes, respectively, drawing inspiration from the dimensionality reduction capabilities inherent to L1 and L2 norms. In contradistinction to the point-to-point distance metric, the class-to-point distance measure is assessed using the assumption. It is regarded as the embedding framework's straightforward and reliable approach for dimensionality reduction. Equation (13) expresses the objective function as follows:

$$w_{opt} = \arg\max_{w^T w=1} \frac{\sum_{i,j=1}^{c} B_{ij} \left\| w^T (m_i - m_j) \right\|_2^2}{\sum_{k=1}^{c} \sum_{i,j=1}^{N_k} A_{i,j}^k \left\| w^T (x_i^k - x_j^k) \right\|_2^2} = \arg\max_{W^T W = I_d} \frac{\| w^T X_b \|_{2,1}}{\| w^T X_w \|_{2,1}} \quad (13)$$

Here, the L_2,1 norm of a matrix is specified by 〖‖.‖〗_2,1. Compared to standard norm-1 and norm-2, the precision of the L2,1 is higher. L_2,1 displays the same average classification accuracy in the absence of noise in training data. The average classification accuracy is reduced when PCOS samples are present in the training data.

3.5. Bounding box-CNN with Image Samples

Consider a collection of images denoted I = {I_1, …, I_N}, each accompanied by a corresponding set of bounding boxes B = {B_1, …, B_N}make up the provided dataset size 'N'. The configuration of the network is accomplished through the application of object segmentation techniques. In this case, BB-CNN is used with the parameters to classify the foreground and background of the images' central region. The suggested BB-CNN model is easy to configure and comprehend. It consists of two net has conv layers, max-pool layers, and it uses ReLU. In order to preserve the input size, the convolutional layer pads out with zero after reducing the output layer by half the kernel size. Dense neuron layers connect the pooling and convolutional layers, and the output is connected to the foreground and background pictures. In order to achieve regularization and in order to mitigate overfitting issues, dropout regularisation has been incorporated into both the output layer and the preceding dense layer. To mitigate the issue of class imbalance, an equal number of samples, specifically K=10^5 patches, were drawn from the training dataset encompassing all classes, namely foreground and background photographic images. For a predetermined number of epochs, the weights are initialized utilising a Gaussian distribution, optimisation is performed through adaptive gradient descent, with a specified learning rate of η = 0.0015. As a result, it offers robustness and quicker convergence. Cross-entropy between the encoding factors is used to evaluate the loss function. Every cycle of BB-CNN training updates the target regions. The BB-CNN model's iterative structure yields possess theoretical guarantees of global optimality, though implementation often restricts convergence to local optima neighbourhoods. As a result, the final region-based segmentation depends on the original areas. The bounding box coordinates more accurately and produces better results since the procedure is closer to the items. The following is a discussion of the suggested BB-CNN's pseudo-code :

Pseudo code 1: BB-CNN

Input: training input, i.e. $train\_x$; $train\_y$; $test\_x$; and $test\_y$;
Output: weight and bias; $Sample_{smoot}$ (x);
Parameters: Bounding boxes $B = \{B_1, \ldots, B_N\}$; learning rate = 0.001; error rate; Loss function;
Initialize weight and bias
Begin:
1: Initialize; //'zero centre' normalization, padding, cross-entropy (network configuration);
2: Compute bounding box coordinates;
3: ***while*** $f_{loss} = loss_{intermediate\ layers}$;
4: ***for all*** training set;
5: $\boldsymbol{train\_x}$ and $\boldsymbol{train\_y}$; //label prediction
6: ***end for***
7: Compute smoothing region (x);
8: Compute the binary loss function, L_(binary loss), predicated on the 'class norm' and 'region norm' values
9: Delineate a central region of interest via pixel coordinates (x_0, y_0) and (x_1, y_1);
10: Attain classified output;
11: ***end while***
12: ***End***

4. NUMERICAL RESULTS AND DISCUSSION

This section presents the anticipated experimental results of the model, obtained via simulation in the MATLAB 2020a environment on a personal computer equipped with an i5 processor operating at 1.90 GHz and possessing 4 GB of RAM. Correctness, precision, recall, and the F-value are some performance indicators used for prediction. The confusion matrix serves as the foundation for deriving performance metrics. Here, T.P. denotes the count of instances predicted to be positive that were in fact positive; T.N. indicates confusion matrix underpins performance indicators: TP = predicted positive, actually positive; TN = predicted negative, actually negative; F.N. indicates the number of

ISSN: 1992-8645 www.jatit.org E-ISSN: 1817-3195

positive situations that are meant to be negative, while F.P. indicates the quantity of instances which are genuinely negative yet were predicted to belong to the positive class. In this case, the model's capability to process the entirety of an instance as either positive or negative determines the forecast accuracy. It is said as follows:

$$Prediction\ accuracy = \frac{(TP+TN)}{(TP+FN+FP+TN)} * 100\% \quad (14)$$

The percentage of correctly predicted positive cases among the complete set of instances for which the predictor model yielded a positive classification is used to illustrate precision. Equation (15) expresses it as follows:

$$Precision = \frac{TP}{(TP+FP)} \quad (15)$$

The percentage of expected positive cases that are always positive is used to illustrate recall. Equation (16) expresses it as follows:

$$Recall = \frac{TP}{(TP+FN)} \quad (16)$$

The measure typically employed for classification difficulties is shown as the the F1 rating. The recall and precision rate are calculated using the average harmonic approach, possessing an upper bound of 1 and a lower bound of 0. Equation (17) provides a mathematical expression for it.

$$F1-score = 2 * \frac{precision * recall}{precision + recall} \quad (17)$$

The number of features categorized wrongly, compared to how many there were total of features is used to illustrate the misclassification rate. Equation (18) expresses it as follows:

$$Misclassification\ rate = \frac{Number\ of\ features\ classified\ incorrectl}{Total\ number\ of\ features} \quad (18)$$

Table 3 : Performance comparisons various CNN methods

Dataset	ML algorithm	Precision (%)	F1-score	Accuracy (%)	Recall (%)	AUROC	Misclassification rate
Kaggle dataset	Hybrid CNN and NADE	0.75	0.15	92.60	0.73	92.90	0.15
	CNN	0.80	0.15	87.90	0.70	92.39	0.14
	CNN and KELM	0.75	0.15	88.95	0.75	93.88	0.80
	Deep CNN with data augmentation	0.76	0.19	86.79	0.75	91.45	6.82
	CNN and Genetic Algorithm	0.89	0.19	87.90	0.94	92.34	1.100
	Standard CNN	0.93	0.19	93.15	0.94	95.90	0.09
	Proposed BB − CNN	**0.94**	**0.25**	**95.89**	**0.98**	**96.80**	**0.05**
Open-source dataset	Hybrid CNN and NADE	0.75	0.15	90.15	0.70	91.60	0.06
	CNN	0.78	0.15	91.15	0.69	91.17	0.09
	CNN and KELM	0.79	0.15	90.40	0.70	90.16	0.80
	Deep CNN with data augmentation	0.77	0.15	91.85	0.69	89.40	6.09
	CNN and Genetic Algorithm	0.72	0.15	90.15	0.75	91.100	1.65
	Standard CNN	0.95	0.24	93.16	0.94	92.60	0.09
	Proposed BB − CNN	**0.93**	**0.29**	**95.60**	**0.95**	**93.60**	**0.05**
Constructive dataset for PCOS	Hybrid CNN and NADE	79.2	89.25	95	76.8	86	1.25
	CNN	60	67	96.13	75	85.5	2.658
	CNN and KELM	83.4	72	93.6	76.5	84	4.56
	Deep CNN with data augmentation	81.2	77.9	94.58	75	80	3.56

ISSN: 1992-8645 www.jatit.org E-ISSN: 1817-3195

	CNN and Genetic Algorithm	91.97	94.24	94.2	96.62	78	4.57
	Standard CNN	89.56	90	90.1	85	89	2.89
	Proposed BB − CNN	**93.79**	**95.65**	**97.31**	**97**	**91**	**0.04**

The overall comparison of the planned and current techniques is shown in Table 4. The efficacy of the model put forth is assessed using popular techniques such as CNN+NADE hybrid, plain CNN, CNN+KELM, deep CNN with extra synthetic data (data augmentation), CNN optimised with genetic algo (CNN+GA), and just a regular CNN in the context of the Kaggle dataset for PCOS classification. With a precision of 95.87%, the predicted model outperforms other methods by 3.33%, 8%, 6.89%, 9.11%, 8%, and 2.73%. The expected model's reliability is 91%, which is 17%, 14%, 20%, 17%, 6%, and 1% better than previous methods. With a recall of 94%, the expected model outperforms other methods by 24%, 26%, 23%, 22%, 5%, and 2%. The expected model has an F1-score of 20, which is significantly higher than other methods. With a 96.78% AUROC, the expected model's execution time of 0.04 minutes is significantly better. The predicted model's accuracy in the open MRI dataset is 95.56%, which is 5.43%, 4.44%, 5.17%, 3.67%, 5.43%, and 2.41% greater than previous methods. The expected model's precision is 92%, which is 19%, 17%, 16%, 18%, 22%, and 1% better than alternative methods. The expected model has an accuracy of 93%, which is 25%, 26%, 24%, 26%, 22%, and 1% greater than previous methods. The expected model has a f1-score of 24, which is greater than other methods. With 93.58% AUROC, the execution time is 0.04 minutes, better than previous models. The model efficiency for the T1-weighted contrast enhancement M.R. pictures dataset is 97.31%, which is 2.31%, 1.18%, 3.71%, 2.73%, 3.11%, and 7.21% better than other methods. The expected model's reliability is 93.79%, which is greater than other methods by 14.59%, 33.79%, 10.39%, 12.59%, 1.82%, and 4.23%. With an accuracy of 97%, the predicted model outperforms previous methods by 20.2%, 22%, 20.5%, 0.38%, 22%, and 12%. The predicted model has a f1-score of 95.65, which is significantly higher than other methods. With 93.58% AUROC, the execution time is 0.04 minutes, better than previous models. This analysis demonstrates that the pattern performs well across all measures using the given information set.

Table 4: Performance evaluation-based on the data partition

Metrics	Data Splitting Range (%)	Layered CNN	BB-CNN	CNN
Accuracy	30-70	68.18	72.18	68.27
	35-65	71.95	74.90	72.92
	40-60	74.25	79.46	74.80
	45-55	76.78	82.50	78.97
	50-50	80.01	86.55	81.08
	55-45	83.20	90.12	84.26
	60-50	85.18	93.15	87.97
	65-55	88.98	95.14	92.45
	70-30	92.22	**97.34**	93.57
Precision	30-70	67.25	69.87	69.87
	35-65	69.82	71.25	70.19
	40-60	**70.21**	**74.52**	**72.68**
	45-55	**75.27**	**76.89**	**76.16**
	50-50	**81.97**	**79.81**	**81.02**
	55-45	**84.51**	**83.89**	**85.56**
	60-50	**87.97**	**87.19**	**89.87**
	65-55	**90.02**	**93.68**	**91.71**
	70-30	93.17	**96.01**	94.38
Recall	30-70	69.46	68.97	67.46
	35-65	69.91	72.50	73.15
	40-60	**72.34**	**75.25**	**76.45**
	45-55	**75.96**	**76.15**	**78.25**

ISSN: 1992-8645 www.jatit.org E-ISSN: 1817-3195

	50-50	**80.99**	**78.56**	**81.86**
	55-45	**85.79**	**84.56**	**85.87**
	60-50	**88.78**	**88.98**	**87.89**
	65-55	**91.91**	**94.19**	**91.92**
	70-30	93.17	**96.01**	93.57
F-measure	30-70	72.48	70.21	71.91
	35-65	75.31	73.68	74.65
	40-60	77.45	**74.49**	**77.79**
	45-55	81.26	**77.21**	**80.67**
	50-50	83.13	**79.67**	**84.58**
	55-45	86.03	**84.72**	**87.91**
	60-50	88.19	**89.91**	**90.74**
	65-55	92.57	**93.46**	**92.68**
	70-30	93.17	**96.01**	94.38

a) Input image *b) Pre-processed image* *c) Predicted outcome*

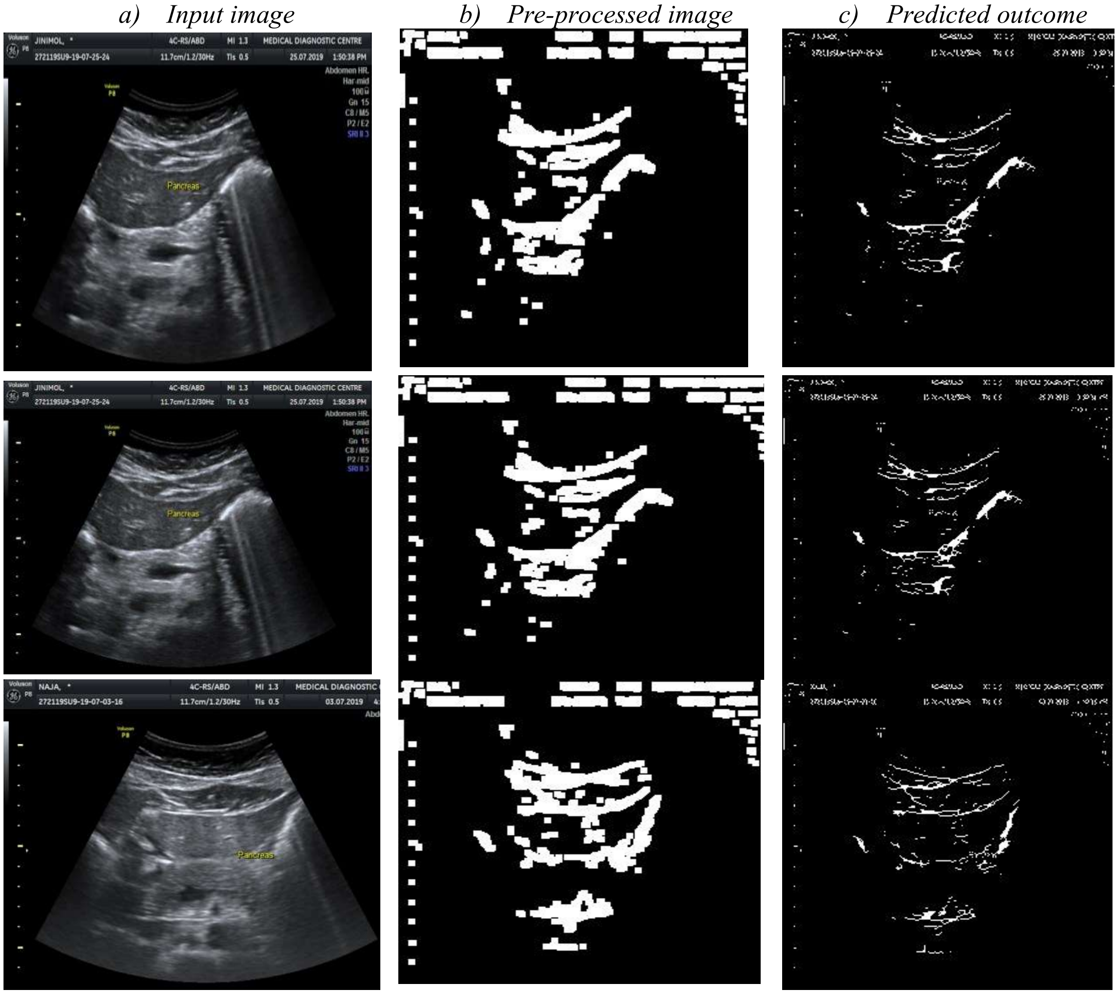

ISSN: 1992-8645 www.jatit.org E-ISSN: 1817-3195

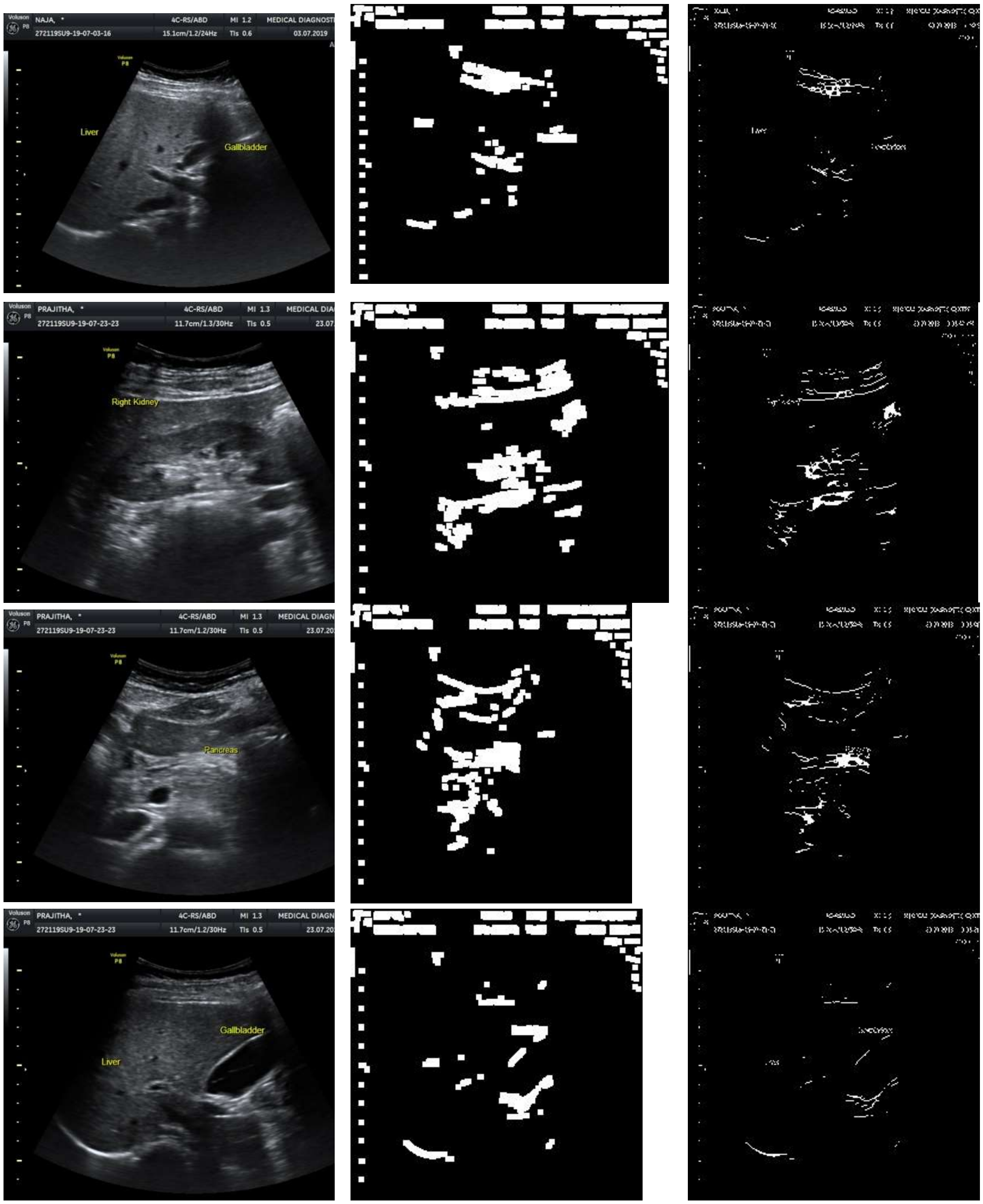

Journal of Theoretical and Applied Information Technology
15st July 2026. Vol.104. No.13

ISSN: 1992-8645 www.jatit.org E-ISSN: 1817-3195

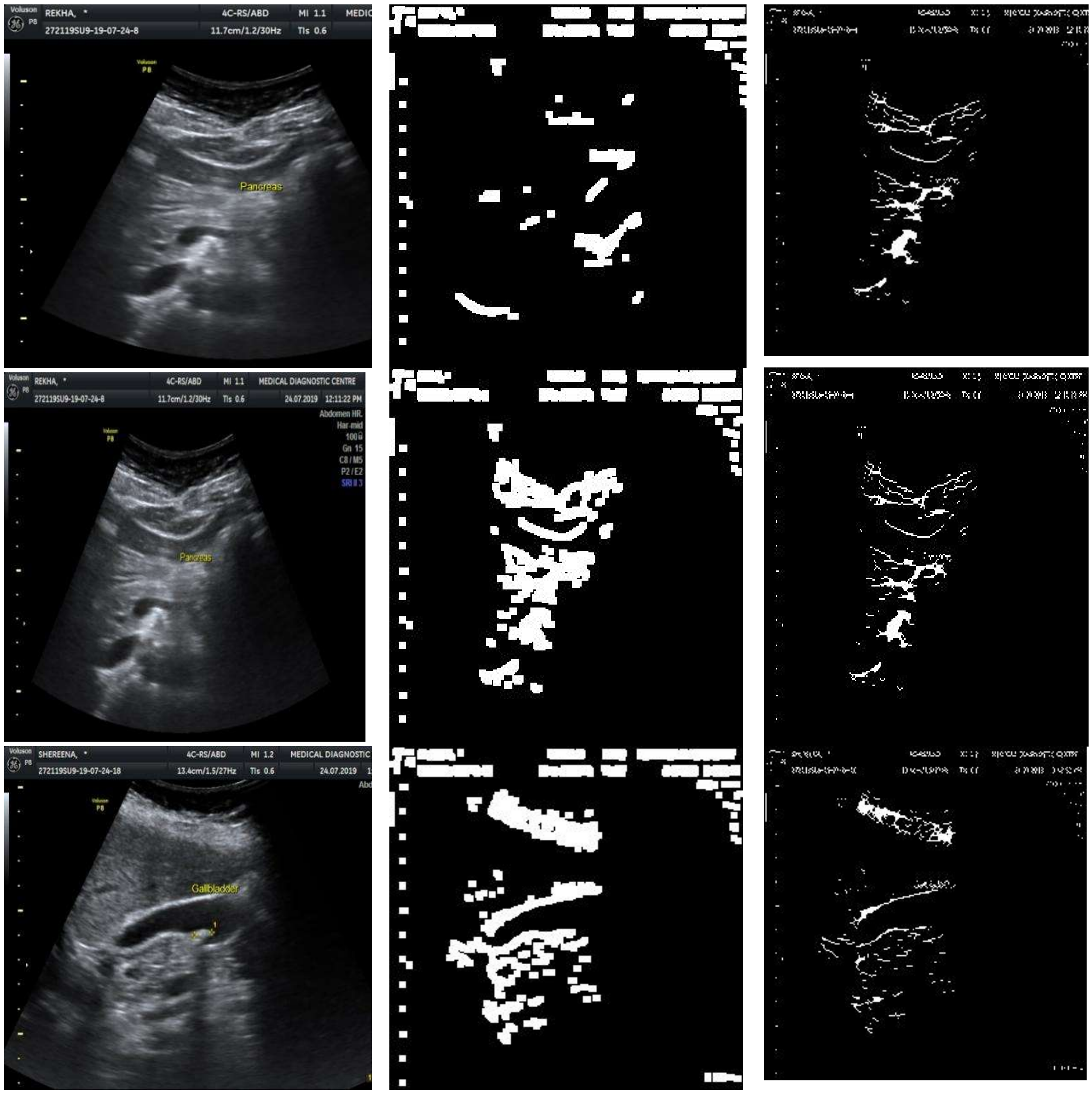

Fig 1: Prediction outcomes

To check how well it performs, we chopped the data into training and testing bits using nine different cuts: testing was 30%, 35%, 40%, 45%, 50%, 55%, 60%, 65%, 70% -- with training making up the rest. With a prediction accuracy of 97.34%, the suggested model significantly outperforms CNN and layered CNN. In this case, 30% of the data allocation comprises 30% devoted to testing and 70% utilised for training purposes. In a same vein, BB-CNN outperforms CNN and layered CNN with accuracy, recollections, and the F1 statistic of 96.01%. In addition to 70:30, the model performs better at 30:70, 35:65, 40:60, 45:55, 50:50, 55:45, 60:50, 65:55, and 70:30. For 70% training and 30% testing samples, BB-CNN's prediction accuracy is 97.34%, 3.77% and 5.12% higher than CNN and layered CNN, respectively. Utilising a training set comprising 70% of samples and a testing set of 30%, the BB-CNN model demonstrates a precision of 96.01%,1.63% and 2.84% higher than CNN and layered CNN, respectively. For 70% training and 30% testing samples, BB-CNN has a recall of 96.01%, which is 2.44% and 2.84% higher than CNN and layered CNN. In the scenario where 70% of samples are allocated to the training set and 30% to the testing set, the F-measure of BB-CNN is 96.01%, 1.63% and 2.84% higher than CNN and layered CNN, respectively (see Figs. 2 to 5). These analyses clearly show that the model effectively predicts PCOS, as seen in Fig. 1.

Table 5: P-value computation

Features	P-value	Reference value	Parameters
F_1	0.050	18-45	Age
F_7	0.080	38.5±4.4	Testosterone (ng/dl)[a]
F_8	0.075	2.2±0.2	Androstenedione
F_9	0.35	13.1±1.3	Average ovarian volume (ml)
F_{10}	< 0.06	11.7±0.6	No of follicles
F_{11}	< 0.06	6.3±0.4	Endometrial thickness (mm)
F_{12}	< 0.0001	7 (3-10)	Ferriman-Gallwey
F_{13}	0.25	23.9±0.9	BMI (kg/m^2)
F_{14}	0.50	38	Obesity
F_{15}	0.003	2.3	Free Testosterone (pg/dl)

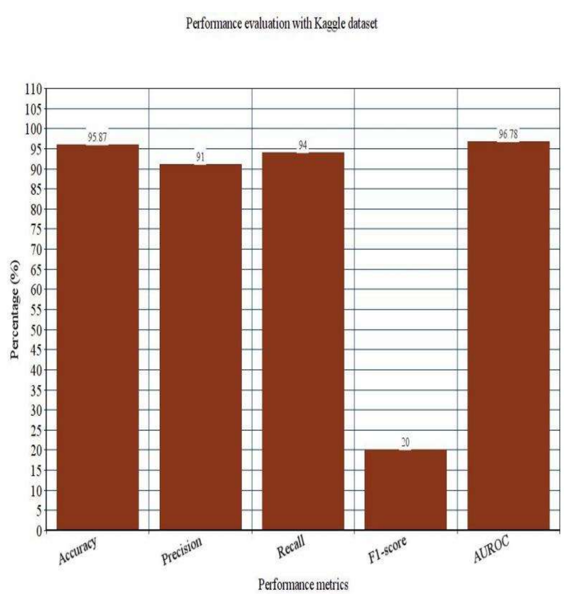

Fig 2 Performance evaluation with Kaggle dataset

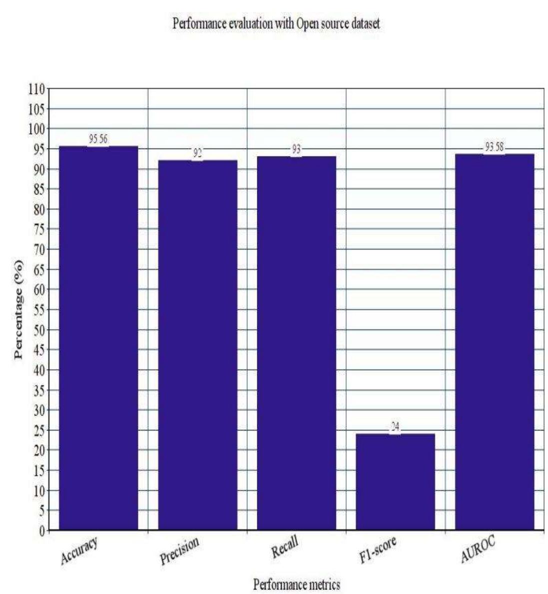

Fig 3 Performance evaluation with Open source dataset

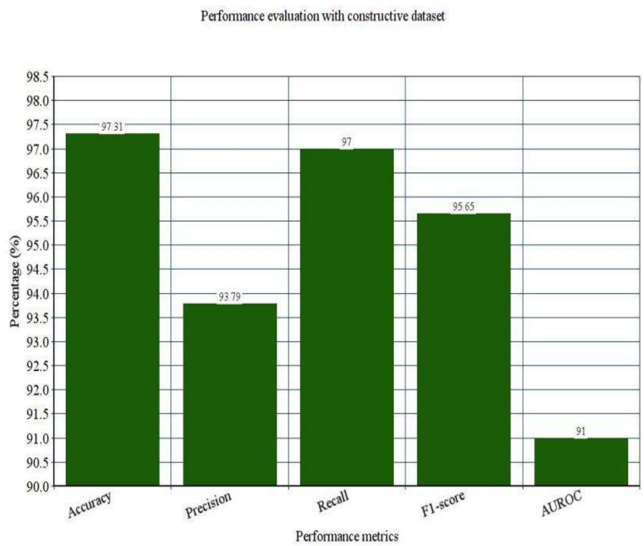

Fig 4 Performance evaluation with the constructive dataset

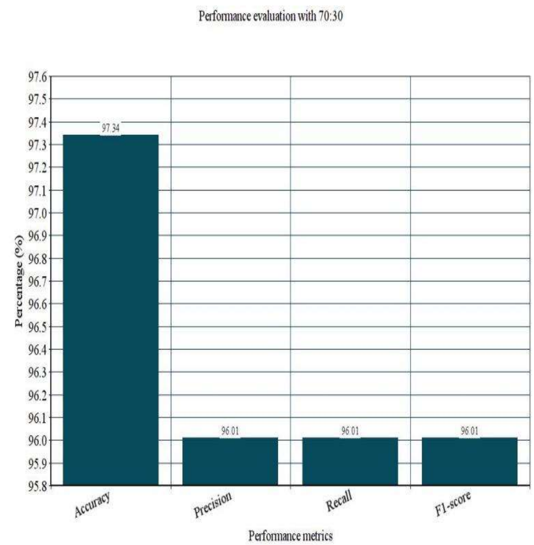

Fig 5 Performance evaluation with 70:30 data

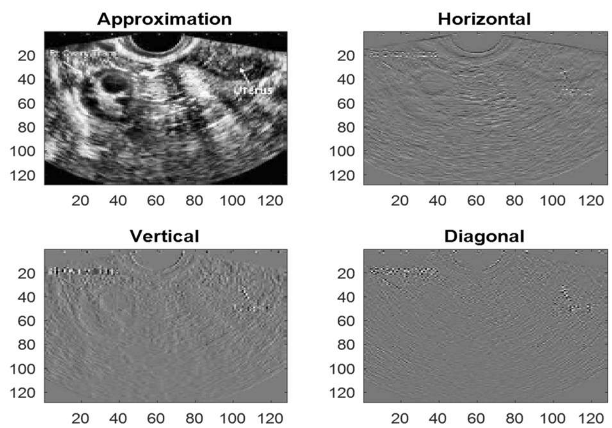

Fig 6 Sample approximation

4.1. Statistical Analysis

Unlike the point-to-point distance metric, the class-to-point distance measure is used to assess the application of statistical methodologies of the suggested model. The BB-CNN model and the traditional model's performance scores are compared, and the disparities between them are normalized between [0, 1]. As shown in Table 5, the suggested model's p-value is greater than that of the traditional model. As a result, this model is regarded as an effective model for PCOS prediction. The suggested model effectively predicts PCOS if the p-value is less than 1. The sampling approximation of the expected model is shown in Fig. 6.

5. CONCLUSION

The aim is to develop a PCOS detection model using machine learning methods. To get better accuracy and lower data dimensionality, feature selection is first carried out. Here, an online dataset has been taken into consideration for computation, and L_2,1 normalization is used to evaluate feature vectors. When these successive characteristics are fed into the classifier model, the chosen features are taken into account. Here, a brand-new BB-CNN model that functions as a clinical decision model is suggested using the bounding box computation. Based on class labels, where "0" indicates negative computation and "1" indicates positive computation, this approach successfully produces superior classification results. Metrics including accuracy, specificity, precision, recall, and F-measure are

ISSN: 1992-8645 www.jatit.org E-ISSN: 1817-3195

assessed in order to validate this result. The training values improve decision-making for clinical measurements and demonstrate more accuracy in predicting PCOS.

REFERENCES

[1] Abelson, S, Collord, G, Ng, SW, Weissbrod, O, Cohen, NM, Niemeyer, E, Barda, N, Zuzarte, PC, Heisler, L &Sundaravadanam, Y 2018, 'Prediction of acute myeloid leukaemia risk in healthy individuals, nature, vol. 559, no. 7714, pp. 400-404.

[2] Babaoglu, I, Baykan, OK, Aygul, N, Ozdemir, K &Bayrak, M 2009, 'Assessment of exercise stress testing with artificial neural network in determining coronary artery disease and predicting lesion localization', Expert Systems with Applications, vol. 36, no. 2, pp. 2562-2566.

[3] Bellver, J, Ayllón, Y, Ferrando, M, Melo, M, Goyri, E, Pellicer, A, Remohí, J &Meseguer, M 2010, 'Female obesity impairs in vitro fertilization outcome without affecting embryo quality', Fertility and sterility, vol. 93, no. 2, pp. 447-454.

[4] Brasko, C, Smith, K, Molnar, C, Farago, N, Hegedus, L, Blind, A, Balassa, T, Szkalisity, A, Sukosd, F &Kocsis, K 2018, 'Intelligent image-based in situ single-cell isolation', Nature Communications, vol. 9, no. 1, pp. 1-7.

[5] Chen, Y, Nisenblat, V, Yang, P, Zhang, X & Ma, C 2018, 'Reproductive outcomes in women with unicornuate uterus undergoing in vitro fertilization: a nested case-control retrospective study', Reproductive Biology and Endocrinology, vol. 16, no. 1, p. 64.

[6] De Kat, AC, van der Schouw, Y, Eijkemans, M, Herber-Gast, G, Visser, J, Verschuren, W &Broekmans, F 2016, 'Back to the basics of ovarian aging: a population-based study on longitudinal anti-Müllerian hormone decline', BMC medicine, vol. 14, no. 1, p. 151.

[7] Dumesic, DA, Oberfield, SE, Stener-Victorin, E, Marshall, JC, Laven, JS &Legro, RS 2015, 'Scientific statement on the diagnostic criteria, epidemiology, pathophysiology, and molecular genetics of polyic ovary syndrome', Endocrine Reviews, vol. 36, no. 5, pp. 487-525.

[8] Hornstein, MD 2016, 'State of the ART: assisted reproductive technologies in the United States, Reproductive Sciences, vol. 23, no. 12, pp. 1630-1633.

[9] Jones, MR &Goodarzi, MO 2016, 'Genetic determinants of polyic ovary syndrome: progress and future directions', Fertility and sterility, vol. 106, no. 1, pp. 25-32.

[10] Legro, RS, Brzyski, RG, Diamond, MP, Coutifaris, C, Schlaff, WD, Casson, P, Christman, GM, Huang, H, Yan, Q &Alvero, R 2014, 'Letrozole versus clomiphene for infertility in the polyic ovary syndrome', N Engl J Med, vol. 371, pp. 119-129.

[11] Mary, MJ, Vetrivel, U, Munuswamy, D &Melanathuru, V 2016, 'PCOSDB: Polyic Ovary Syndrome Database for manually curated disease associated genes', Bioinformation, vol. 12, no. 1, p. 4.

[12] Moschos, E &Twickler, DM 2015, 'Prediction of polyic ovarian syndrome based on ultrasound findings and clinical parameters', Journal of Clinical Ultrasound, vol. 43, no. 3, pp. 157-163.

[13] Peng, C, Zou, L & Huang, D-S 2018, 'Discovery of relationships between long non-coding RNAs and genes in human diseases based on tensor completion', IEEE Access, vol. 6, pp. 59152-59162.

[14] Perry, DS, Gunawardena, J &Orsi, N 2018, 'Identification of Non-invasive Cytokine Biomarkers for Polyic Ovary Syndrome Using Supervised Machine Learning, in Proceedings of the 2018 ACM International Conference on Bioinformatics, Computational Biology, and Health Informatics, pp. 502-502.

[15] Ramy, MH, El-Beltagy, M, Saleh, M & Mostafa, B 2012, 'A hybridized approach for feature selection using ant colony optimization and ant-miner for classification', in 2012 8th International Conference on Informatics and Systems (INFOS), pp. BIO-211-BIO-219.

[16] Sarfraz, S &Nezamabadi-pour, H 2013, 'Facing the classification of binary problems with a GSA-SVM hybrid system', Mathematical and Computer Modelling, vol. 57, no. 1-2, pp. 270-278.

[17] Sarfraz, S &Nezamabadi-pour, H 2013, 'Facing the classification of binary problems with a GSA-SVM hybrid system', Mathematical and Computer Modelling, vol. 57, no. 1-2, pp. 270-278.

[18] Sharif, E, Rahman, S, Zia, Y &Rizk, NM 2017, 'The frequency of polyic ovary syndrome in young reproductive females in Qatar', International journal of women's health, vol. 9, p. 1.

[19] Smoot, ME, Ono, K, Ruscheinski, J, Wang, P-L &Ideker, T 2011, 'Cytoscape 2.8: new features for data integration and network visualization', Bioinformatics, vol. 27, no. 3, pp. 431-432.
[20] Uyar, A, Bener, A &Ciray, HN 2015, 'Predictive modeling of implantation outcome in an in vitro fertilization setting: an application of machine learning methods', Medical Decision Making, vol. 35, no. 6, pp. 714-725.
[21] Vieira, SM, Mendonça, LF, Farinha, GJ & Sousa, JM 2013, 'Modified binary PSO for feature selection using SVM applied to mortality prediction of septic patients', Applied Soft Computing, vol. 13, no. 8, pp. 3494-3504.
[22] Welt, CK & Duran, JM 2014, 'The genetics of polyic ovary syndrome', in Seminars in reproductive medicine, vol. 32, p. 177.
[23] Yanez, LZ, Han, J, Behr, BB, Pera, RAR & Camarillo, DB 2016, 'Human oocyte developmental potential is predicted by mechanical properties within hours after fertilization, Nature communications, vol. 7, no. 1, pp. 1-12.
[24] Zandi, S, Farajzadeh, S & Safari, H 2016, 'Prevalence of polyic ovary syndrome in women with acne: hormone profiles and clinical findings', Journal of Pakistan Association of Dermatology, vol. 20, no. 4, pp. 194-198.
[25] Yildiz, BO, Bozdag, G, Yapici, Z, Esinler, I &Yarali, H 2012, 'Prevalence, phenotype and cardiometabolic risk of polyic ovary syndrome under different diagnostic criteria, Human reproduction, vol. 27, no. 10, pp. 3067-3073.